Vilà-González *et al. Respiratory Research* (2024) 25:180
https://doi.org/10.1186/s12931-024-02800-7

Respiratory Research

RESEARCH

Open Access

In vitro platform to model the function of ionocytes in the human airway epithelium

Marta Vilà-González[1,15,16*], Laetitia Pinte[1], Ricardo Fradique[2], Erika Causa[2], Heleen Kool[3], Mayuree Rodrat[4,5], Carola Maria Morell[1,6], Maha Al-Thani[7], Linsey Porter[8], Wenrui Guo[8], Ruhina Maeshima[9], Stephen L. Hart[9], Frank McCaughan[8], Alessandra Granata[7], David N. Sheppard[4], R. Andres Floto[10,11], Emma L. Rawlins[3,12], Pietro Cicuta[2] and Ludovic Vallier[1,13,14*]

Abstract

Background Pulmonary ionocytes have been identified in the airway epithelium as a small population of ion transporting cells expressing high levels of *CFTR* (cystic fibrosis transmembrane conductance regulator), the gene mutated in cystic fibrosis. By providing an infinite source of airway epithelial cells (AECs), the use of human induced pluripotent stem cells (hiPSCs) could overcome some challenges of studying ionocytes. However, the production of AEC epithelia containing ionocytes from hiPSCs has proven difficult. Here, we present a platform to produce hiPSC-derived AECs (hiPSC-AECs) including ionocytes and investigate their role in the airway epithelium.

Methods hiPSCs were differentiated into lung progenitors, which were expanded as 3D organoids and matured by air-liquid interface culture as polarised hiPSC-AEC epithelia. Using CRISPR/Cas9 technology, we generated a hiPSCs knockout (KO) for *FOXI1*, a transcription factor that is essential for ionocyte specification. Differences between *FOXI1* KO hiPSC-AECs and their wild-type (WT) isogenic controls were investigated by assessing gene and protein expression, epithelial composition, cilia coverage and motility, pH and transepithelial barrier properties.

Results Mature hiPSC-AEC epithelia contained basal cells, secretory cells, ciliated cells with motile cilia, pulmonary neuroendocrine cells (PNECs) and ionocytes. There was no difference between *FOXI1* WT and KO hiPSCs in terms of their capacity to differentiate into airway progenitors. However, *FOXI1* KO led to mature hiPSC-AEC epithelia without ionocytes with reduced capacity to produce ciliated cells.

Conclusion Our results suggest that ionocytes could have role beyond transepithelial ion transport by regulating epithelial properties and homeostasis in the airway epithelium.

Keywords Airway epithelium, Ionocytes, Human induced pluripotent stem cells, Tissue modelling, FOXI1

*Correspondence:
Marta Vilà-González
mv468@cam.ac.uk; marta.vila@ssib.es
Ludovic Vallier
ludovic.vallier@bih-charite.de

Full list of author information is available at the end of the article

Background

Pulmonary ionocytes were described in 2018 as a small population of airway epithelial cells (AECs) that express high levels of ion channels and transporters, including CFTR (cystic fibrosis transmembrane conductance regulator), the protein mutated in cystic fibrosis (CF) [1–3]. Thus, it has been hypothesised that ionocytes might have a role in the pathogenesis of CF and understanding their function could be key in identifying new therapies for CF and other respiratory diseases. So far, available information on ionocytes and their function in the human airway epithelium is limited. Specific markers for this cell type include FOXI1 (forkhead box I1), high CFTR expression, ASCL3 (achaete-scute family BHLH transcription factor 3) and STAP1 (signal transducing adaptor family member 1) [2]. Ionocytes also express high levels of the vacuolar H^+ ATP-ase (VATPase), barttin (BSND)/ClC-K channels and the large conductance Ca^{2+}-activated K^+ channel ($K_{Ca}1.1$) [2]. They seem to be more abundant in the nasal epithelium and proximal airways [4, 5] where they are more commonly found in the ducts of submucosal glands [3].

Lineage tracing analysis suggests that ionocytes differentiate from basal cells [2]. By showing that knock out (KO) of *POU2F3* leads to air liquid interface (ALI) cultures with decreased numbers of ionocytes and pulmonary neuroendocrine cells (PNECs), Goldfarbmuren et al. [6] suggested that tuft cells give rise to both ionocytes and PNECs. By contrast, Plasschaert et al. [1] showed that the transcription factor *FOXI1* is sufficient to drive ionocyte differentiation, while the inhibition of Notch signalling in ALI cultures leads to a reduction in their number. This pathway for ionocyte differentiation seems to be conserved between species [7]. More recently, Wang et al. [8] reported no changes in ionocyte marker expression after they overexpressed *NOTCH* in AECs derived from human induced pluripotent stem cell (hiPSCs). This could indicate that lower levels of Notch signalling are needed for ionocyte specification than those required by secretory cells and that signalling is finely tuned to achieve the complex composition of the airway epithelium [9–11]. Finally, Cai et al. [12] demonstrated that the Sonic hedgehog pathway is involved in ionocyte specification by showing that the inhibition of this pathway reduces the amount of ionocytes in culture, while its activation using the chemical agonist SAG (Sonic hedgehog agonist) increases their numbers. Thus, cross-talk between these two signalling pathways seems to be involved in ionocyte specification.

Early studies of the function of ionocytes by Plasschaert et al. showed that reduction of the number of ionocytes could affect CFTR-mediated Cl^- currents in Ussing chamber assays [1], which was recently verified by the study of Cai et al. [12]. Additionally, a more recent study demonstrated ionocyte-specific regulation of CFTR by the phosphodiesterase PDE1C [13]. In a *Foxi1* KO mouse model, absence of Foxi1 led to higher mucus viscosity and ciliary beat frequency (CBF), indicating that ionocytes could have a role in regulating airway physiology [2]. This has been further studied in a recent report by Lei et al. [14]. , where they describe a role of ionocytes in fluid and electrolyte absorption, and in a study by Yuan et al. [15] that demonstrates a pivotal role for ionocytes in homeostatic mechanisms regulating airway surface liquid (ASL) volume, pH and viscosity and mucociliary clearance. Furthermore, the observation that ionocytes have cellular extensions [2, 16], suggests the hypothesis that they could interact directly with other AEC types. However, the precise mechanisms by which ionocytes control these multiple functions are still not fully understood.

The challenge to further understand ionocyte function in human lungs is aggravated by the lack of appropriate models and the limited availability of primary tissue. AECs derived from hiPSCs (hiPSC-AECs) could provide unique opportunities for respiratory research since hiPSCs can grow indefinitely while maintaining their capacity to differentiate into any cell type. However, the differentiation of hiPSCs into AECs lacks standardised protocols and different methods often lead to divergent results [17–19]. Until recently, protocols failed to consistently produce rare AECs such as ionocytes [18]. Hor et al. published a protocol to generate PNECs from hiPSCs in vitro, without identifying ionocytes in their cultures [20]. In a recent report, Wang et al. [8] identified ionocytes in their hiPSC-AEC cultures using a protocol with 3 sorting steps which extended the length of the protocol to almost 80 days. Here, we present a platform to study the role of ionocytes in the airway epithelium in vitro using hiPSCs. We describe a protocol which produces AECs including ionocytes within 60 days and then perform loss of function experiments. Our results show that the KO of FOXI1 in hiPSCs using CRISPR/Cas9 reduced the number of ciliated cells after hiPSC-AEC maturation, indicating that ionocytes could be important in lung lineage specification and homeostasis.

Methods

Full descriptions of the methods used to differentiate hiPSCs into AECs and evaluate them biochemically and functionally are provided in the Supplementary Materials and Methods.

hiPSC differentiation to AECs

To derive AECs from hiPSCs, we used FS13B hiPSC lines generated as described previously [21] and the CF17/NKX2.1-GFP hiPSC line (kindly gifted by UTHEALTH and Dr. Jed Mahoney, Cystic Fibrosis Foundation lab, Lexington, MA, USA). hiPSCs were differentiated by driving cells through definitive endoderm and anterior foregut endoderm to reach a lung progenitor state. At day 16 of differentiation, cells were sorted to enrich for NKX2.1 expressing progenitors using anti-carboxypeptidase-M (CPM) antibody [17], anti-CD26/anti-CD47 sorting strategy [22] or sorting for GFP: NKX2.1 reporter cells [18]. Sorted cells were seeded in 3D Matrigel domes for expansion and cryopreservation. After at least 8 days of growth under expansion conditions, cells were seeded on Transwell® inserts to form mature polarised airway epithelia. Once cells were confluent in the Transwell®, medium bathing the apical membrane was removed to form an ALI. After 28 days of ALI culture, hiPSC-AEC epithelia were characterised biochemically and functionally.

Analysis of mRNA and protein expression

Reverse transcription-quantitative polymerase chain reaction (RT-qPCR), immunofluorescence staining and Western blotting were performed to characterise mRNA and protein expression at different stages of the protocol and to investigate the effects of *FOXI1* KO.

Lung progenitor transplantation into a mouse model of airway injury

Experiments using a mouse model of airway injury were approved by local ethical review committees and conducted according to Home Office project license PPL PEEE9B8E4 (Emma L. Rawlins, University of Cambridge). For these experiments, 9 male 9-week-old immune-compromised *NOD-scid-IL2rg*$^{-/-}$ (NSG; RRID: IMSR_JAX:005557) mice were used [23, 24]. Mice were treated with 2% polidocanol oropharyngeally and transplanted with a suspension of 1 million GFP+hiPSC-derived lung progenitor cells on the next day. At different time points (1, 7 or 10 days) after cell transplantation, mice were sacrificed and tracheas harvested for wholemount immunofluorescence staining to visualise cells.

CRISPR/Cas9-based*FOXI1*KO and phenotypical assays

Single guide RNA (sgRNA) and CRISPR/Cas9 were used to KO *FOXI1* in hiPSCs. The functional consequences of *FOXI1* KO were evaluated using hiPSC-AEC epithelia and pH and transepithelial resistance (R_t) measurements, high-speed microscopy analysis of ciliary dynamics and Ussing chamber studies of epithelial ion transport.

Statistical analysis

Results are expressed as means ± SD of *n* observations. Statistical analyses were performed either using Prism 9 (GraphPad Software Inc., San Diego, CA, USA) or SigmaPlot 14 (Systat Software Inc., San Jose, CA, USA). The type of statistical analysis performed in each experiment and the number of replicates used are described in the figure legends. Differences were considered statistically significant when $P<0.05$. Significance in each analysis is represented by * $P<0.05$, ** $P<0.01$, *** $P<0.001$, **** $P<0.0001$, ns = not significant.

Results

Method to differentiate hiPSCs into AECs including ionocytes

For this study, we used two different hiPSC lines or genetic backgrounds: the previously described FS13B hiPSCs [21] and the CF17/NKX2.1-GFP, which has a GFP reporter for NKX2.1. We first differentiated these two hiPSCs lines into AECs following a natural path of development including definitive endoderm, anterior foregut endoderm and lung progenitors (Fig. 1A). RT-qPCR analyses confirmed the mRNA expression of specific markers for each stage (Fig. 1B and S1A) and cells formed a characteristic network pattern after 16 days of differentiation (Fig. 1C and D). The resulting lung progenitors were then sorted using anti-CPM staining to enrich for NKX2.1 expressing cells in FS13B cells (Fig. 1E and F) while CF17/NKX2.1-GFP cells were sorted for NKX2.1-GFP expression. To expand lung progenitors, sorted cells were grown as 3D organoids (Fig. 2A) in medium supplemented with the GSK3b inhibitor CHIR-99021, the Rho-associated protein kinase inhibitor Y-27632 and fibroblast growth factor 10 (FGF10). These organoids could be cryopreserved and thawed for further experiments while maintaining the expression of lung progenitor markers (Figure S1B). In some instances, organoids were maintained for up to 8 passages or +6 passages after thawing without losing NKX2.1 expression (Figure S1C). Overall, our approach allowed the production and the expansion of lung progenitors in vitro thereby bypassing the need to systematically differentiate hiPSCs.

AEC maturation was performed by dissociating the organoids and seeding lung progenitors in Transwell® inserts. Once confluent, ALI was established and cells were differentiated for an additional 28 days (Fig. 2B and C). To promote the differentiation of ciliated cells, the Notch pathway inhibitor (2 S)-N-[2(3,5-Difluorophenyl) acetyl]-L-alanyl-2-phenyl-glycine 1,1-Dimethylethyl ester (DAPT) was added to the Maturation Medium for the first 14 days after initiating ALI culture. From day 14, PneumaCult™-ALI (PALI) Medium was used to further promote ciliation. The resulting epithelia showed an increase in the expression of *TP63*, *CFTR*, *FOXJ1*, *MUC5AC* and *SCGB3A2* (Fig. 2D) and maintained expression of epithelial markers (Figure S1D). The presence of basal cells (CK5, p63), secretory cells (MUC5AC, SCGB3A2), ciliated cells (FOXJ1, acetylated tubulin (AcTub)), PNECs (ASCL1, CRP) and ionocytes (FOXI1, CFTR high expression, BSND) was confirmed by immunostaining (Fig. 2E and S1E). Importantly, the epithelium

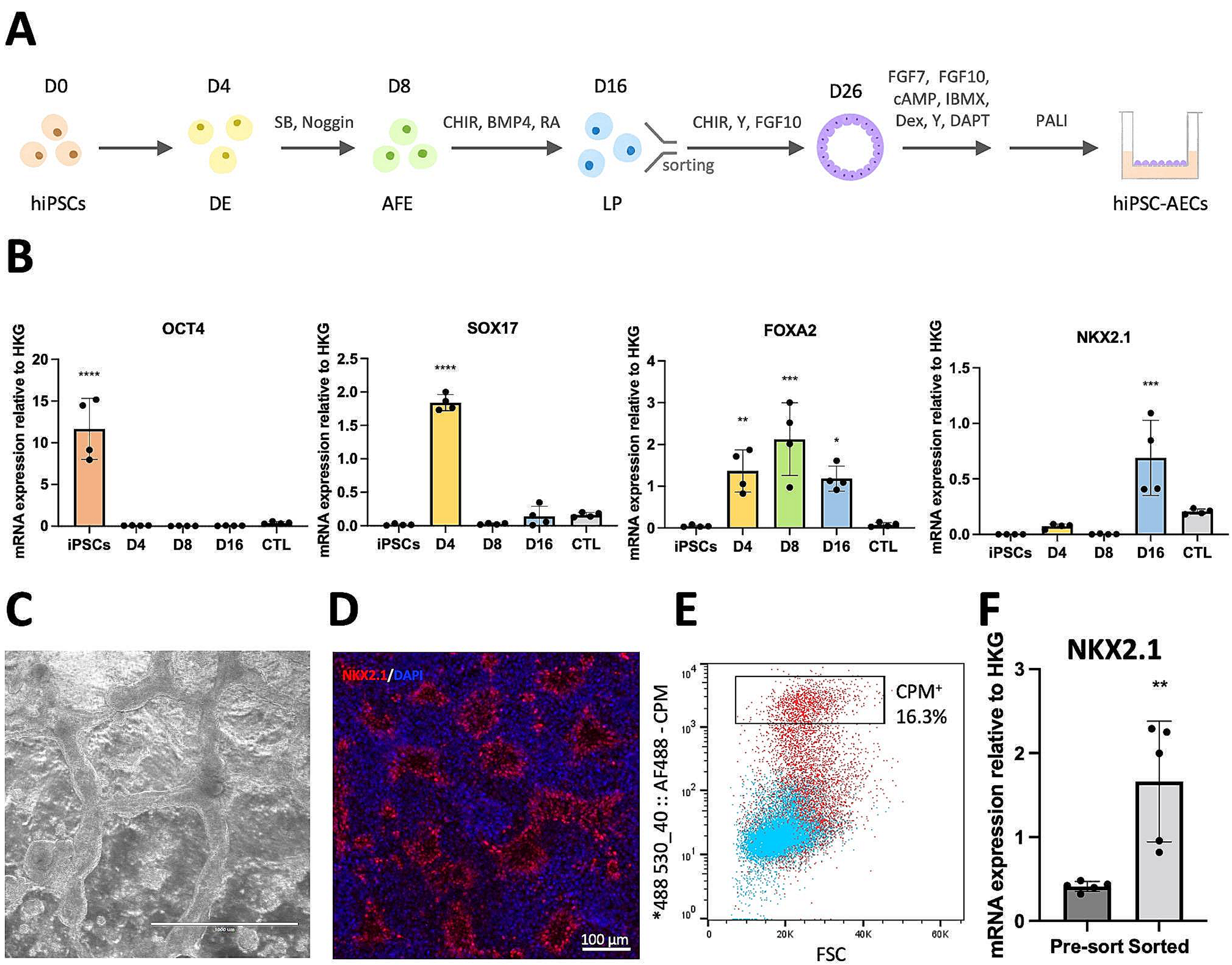

Fig. 1 hiPSCs differentiate into lung progenitors in 16 days. **A**: Diagram of the differentiation protocol, fluorescence activated cell sorting, expansion in 3D organoids and maturation at an ALI to form hiPSC-AECs. Abbreviations: AFE, anterior foregut endoderm; BMP4, bone morphogenetic protein 4; CHIR, CHIR-99021; DAPT, (2 S)-N-[2(3,5-Difluorophenyl)acetyl]-L-alanyl-2-phenyl-glycine 1,1-Dimethylethyl ester; DE, definitive endoderm; FGF7/10, fibroblast growth factor 7/10; IBMX, 3-isobutyl-1-methylxanthine; LP, lung progenitor; PALI, PneumaCult™-ALI Medium; RA, retinoic acid; SB, SB431542; Y, Y-27632. **B**: Relative mRNA expression of key markers at different time points during differentiation. The control (CTL) is human trachea total mRNA. Filled circles represent individual values and columns are means ± SD ($n = 4$ independent experiments). *$P < 0.05$, **$P < 0.01$, ***$P < 0.001$, ****$P < 0.0001$ vs. D0; one-way ANOVA with Tukey's post-test. **C**: Brightfield image of cells after 16 days of differentiation. The scale bar is 1000 µm. **D**: Immunofluorescence staining showing lung progenitor marker NKX2.1 expression (red) and nuclear marker DAPI (blue) on day 16 of differentiation. The scale bar is 100 µm. **E**: Flow cytometry panel showing levels of expression of CPM at day 16 of differentiation (red). The population labelled CPM + was sorted for enrichment of NKX2.1-expressing lung progenitors. HiPSCs stained with anti-CPM antibody served as a negative control (blue). **F**: Enrichment of NKX2.1 mRNA expression after sorting of CPM + cells. Filled circles represent individual values and columns are means ± SD ($n = 5$ independent experiments). **$P < 0.01$ vs. pre-sorted; Student's t-test

was polarised, with cilia (AcTub) located on the apical side and basal cells (CK5) at the basal side of the epithelium (Fig. 2F). Finally, functional analyses confirmed that the hiPSC-AEC epithelium had R_t values comparable to that of primary AECs [25] (Fig. 2G). Analysis of CBF by a robust Fourier Transform method [26], described in the Supplementary Materials and Methods, showed that the cilia in hiPSC-AEC cultures beat at a frequency comparable to that of primary human bronchial epithelial cells (HBECs) (Fig. 2H). The same analysis indicated that hiPSC-AECs were covered by fewer cilia than HBEC cultures (Fig. 2I), consistent with RT-qPCR results for *FOXJ1* expression (Fig. 2D). Taken together, these results show that our protocol allows the production of a polarised airway epithelium containing a diversity of cell types, including ionocytes.

The engraftment capacity of hiPSC-derived lung progenitors

hiPSC-derived lung progenitors have been previously successfully transplanted into the respiratory airways of murine models [27–29], highlighting their potential

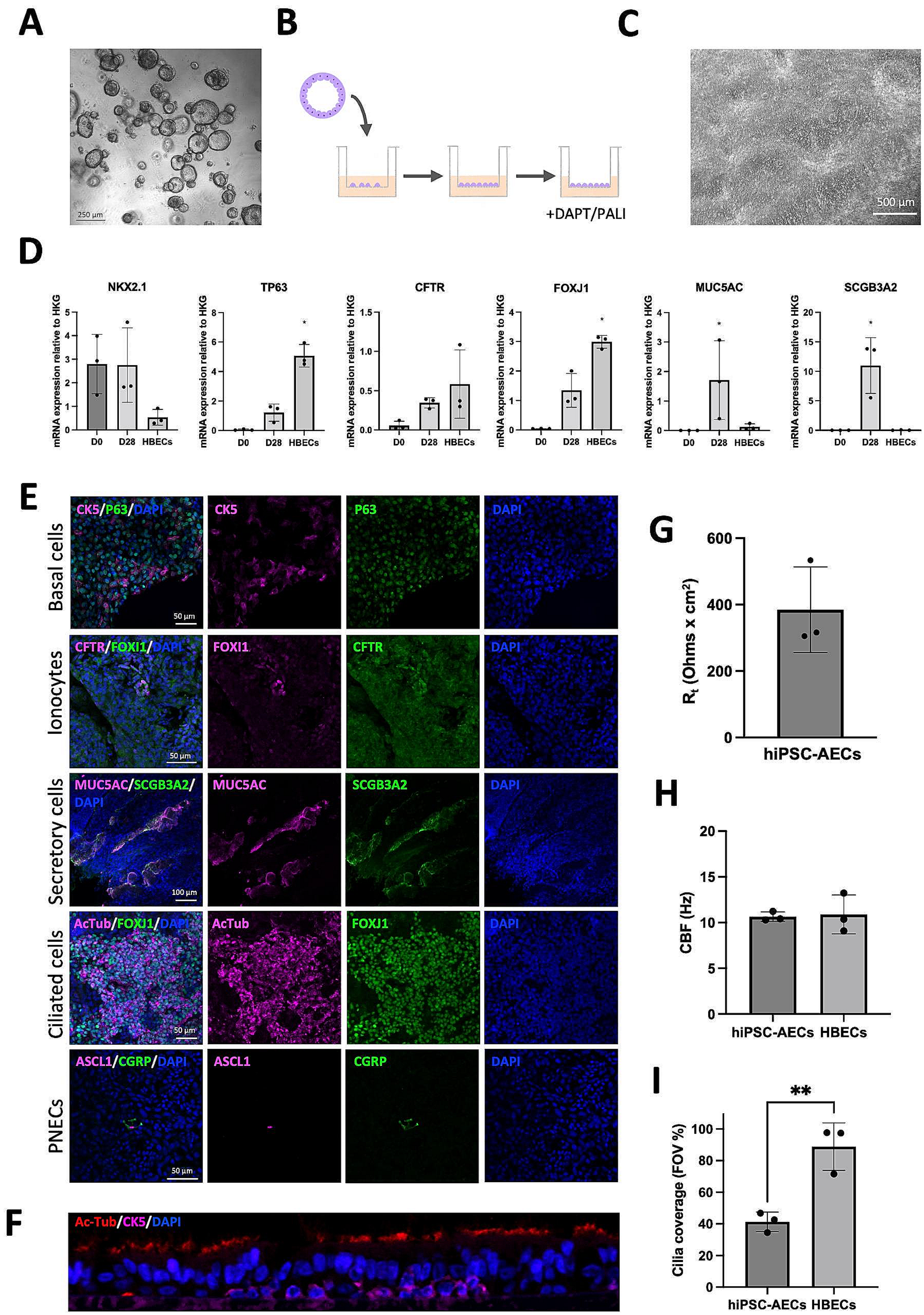

Fig. 2 (See legend on next page.)

(See figure on previous page.)

Fig. 2 ALI culture induces differentiation towards mature AECs with similar properties to HBECs. **A**: Brightfield image of lung progenitors in 3D organoid culture. The scale bar is 250 µm. **B**: Schematic of ALI culture. Organoids were dissociated and cells seeded in Transwell® inserts and cultured with medium on both sides. Once cells were confluent, medium from the top compartment was removed to form an ALI with the apical membrane of cells in contact with air. DAPT was added to the maturation medium in the bottom compartment and the cells cultured for a further 14 days, followed by another 14 days of culture with PALI medium. **C**: Brightfield image of hiPSC-AECs in a Transwell® insert after establishing an ALI. The scale bar is 500 µm. **D**: mRNA expression of AEC markers in cells in expansion conditions (D0) and in ALI culture (D28). ALI cultured HBECs were used as a control. Filled circles represent individual values and columns are means ± SD ($n = 3$ independent experiments); *$P < 0.05$ vs. D0; one-way ANOVA with Tukey's post-test. **E**: Immunocytochemical analysis of mature AEC markers in ALI cultures. The scale bars are 50–100 µm as indicated. **F**: Immunofluorescence staining of a histological section through an ALI culture showing polarization of the airway epithelium. Cilia at the apical side are labelled with Acetylated tubulin (AcTub) and mature basal cells on the basal side are labelled with CK5. **G**: R_t measurements of polarized epithelia formed by hiPSC-AECs. Filled circles represent the average of three readings of the same sample and columns are means ± SD ($n = 3$ independent experiments). **H**: Ciliary beat frequency (CBF) measurements in hiPSC-AECs and HBECs. Filled circles represent the average of 20 FOVs from one sample and columns are means ± SD ($n = 3$ independent experiments); Student's t-test. **I**: Area covered by cilia in hiPSC-AECs ALI cultures is significantly smaller compared to HBECs. Filled circles represent the average of 20 FOVs from one sample and columns are means ± SD ($n = 3$ independent experiments); **$P < 0.01$; Student's t-test

in regenerative medicine. To further demonstrate the functionality of our cells, we explored the engraftment potential of our hiPSC-derived airway progenitors in vivo with a short-term transplantation experiment. We generated lung progenitors from GFP-expressing hiPSC lines (FS13B GFP) and GFP + CPM + sorted cells were cultured as 3D organoids for 8 days before cryopreservation. After thawing and expansion for at least 8 additional days, GFP + organoids expressed similar levels of the lung progenitor and basal cell markers *NKX2.1* and *TP63* when compared to passage 0 organoids (Figure S2A). These organoids were then dissociated into a single cell suspension and 1 million cells were transplanted oropharyngeally into the tracheas of mice that had been topically treated with polidocanol 18 h before transplantation (Fig. 3A). Tracheas were harvested at 1, 7 or 10 days after transplantation and we observed GFP + cells in the tracheas of the 9 mice that had received hiPSC-derived cells (Fig. 3B and Figure S2B). The appearance of clusters of cells indicates that the cells replicated after engraftment (Fig. 3B left). Interestingly, GFP + cells co-expressed CK5 at 7 and 10 days after transplantation (Fig. 3B right), indicating that lung progenitors generated with our approach can not only survive in a mouse model of acute airway injury, but also differentiate towards basal cells. Although longer time points would be needed to assess the full regeneration and differentiation potential of these cells, these results confirm their engraftment capacity.

KO of *FOXI1* in hiPSCs leads to hiPSC-AECs lacking ionocytes

Based on the results generated above, we decided to use our platform to study the importance of ionocytes during the formation of the human airway epithelium. Of note, genetic studies in the mouse have shown that FOXI1 is necessary for the generation of ionocytes in vivo [2]. Thus, we hypothesised that the absence of FOXI1 will stop the production of ionocytes in vitro (Fig. 4A). Using CRISPR/Cas9 genome editing, we generated two hiPSC KOs for the *FOXI1* gene by designing sgRNAs that target the DNA binding domain of *FOXI1*, which is found in exon 1 and is shared by both transcript variants of the gene (Fig. 4B). This approach generated hiPSC lines carrying a loss of function mutation caused by an early stop codon (Figure S3A) as confirmed by genotyping using PCR and Sanger sequencing. Importantly, each of the hiPSC lines was targeted with a different sgRNA to rule out off-target effects, while unedited clones that had gone through the same targeting and clone isolation process were used as isogenic controls (Fig. 4B). The resulting *FOXI1*$^{-/-}$ hiPSCs were then differentiated in parallel with their isogenic wild-type (WT) counterparts. There were no statistically significant differences in the expression of specific markers at key timepoints between the WT and KO up to day 16 of differentiation (Fig. 4C). Thus, the absence of FOXI1 does not affect lung progenitor production. Lung progenitor cells were then enriched by sorting (Fig. 4C) and the resulting organoids were further differentiated using ALI cultures after expansion. After 28 days of culture, WT and KO epithelia showed similar levels of airway markers including *NKX2.1*, *TP63*, *CFTR*, *SCGB3A2*, *FOXJ1* and *MUC5AC* (Fig. 4D). However, the absence of *FOXI1* seemed to induce a limited decrease in the expression of *FOXJ1* in ALI cultures (Fig. 4D and S3B). Of note, we could not detect changes in *FOXI1* expression by RT-qPCR as ionocytes represent only 0.5–1.5% of the epithelium. Immunofluorescence analyses showed the absence of ionocytes in the *FOXI1* KO ALI cultures in contrast to the presence of FOXI1 + CFTR high-expressing ionocytes in WT ALI cultures (Fig. 4E and F). Furthermore, Western blotting indicated absence of FOXI1 protein in *FOXI1* KO ALI cultures compared to its presence in WT epithelia (Fig. 4G and S3C). Together, these data show that *FOXI1* KO leads to hiPSC-AEC epithelia without ionocytes and that their absence does not affect the early differentiation of the lung epithelium.

KO of *FOXI1* reduces ciliation of hiPSC-AECs

We next tested whether the KO of *FOXI1* could affect the function of hiPSC-AECs beyond that of CFTR function, which has already been extensively studied [1, 2, 12–14]. In this study, we first assessed the effect of *FOXI1* KO

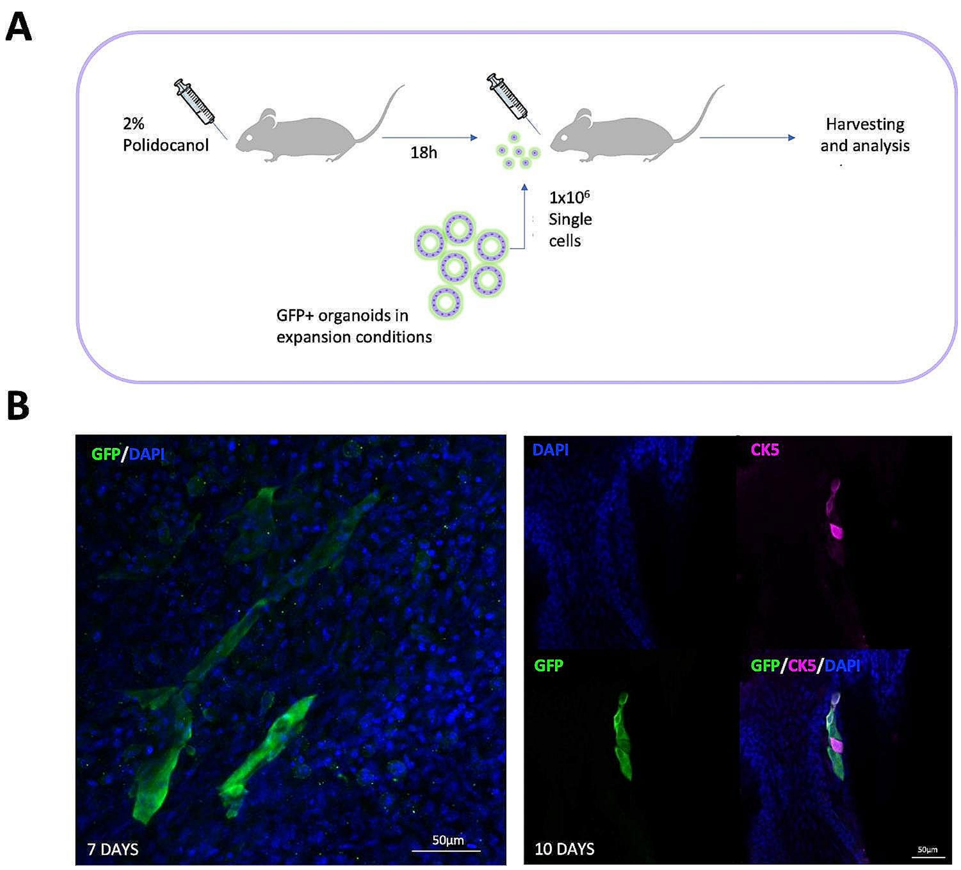

Fig. 3 hiPSC-derived lung progenitors engraft in an in vivo mouse model of airway injury. **A**: Schematic of the cell transplantation procedure. Mice were anesthetized and 30 µl of 2% Polydocanol was administered oropharyngeally. After 18 h, mice were anesthetised again and 30 µl of sterile PBS with 1% BSA and 1 million GFP + hiPSC-derived lung progenitors were administered to the back of the throat. Tracheas were harvested at different time points for analysis. **B**: Representative wholemount immunofluorescence staining showing GFP and DAPI at 7 days after transplantation (left) and GFP, human CK5 and DAPI at 10 days after transplantation (right). The scale bars are 50 µm

on the pH of the ASL in hiPSC-AEC ALI cultures and we confirmed that there were no statistical differences between *FOXI*1 WT and KO cultures (Fig. 5A). We next evaluated whether the KO of *FOXI1* impaired the barrier properties in hiPSC-AEC ALI cultures by measuring R_t. Although *FOXI1* KO epithelia had significantly reduced R_t values compared to those of *FOXI1* WT epithelia (Fig. 5B), Ussing chamber studies revealed that they functionally expressed the epithelial Na^+ channel (ENaC), the Ca^{2+}-activated Cl^- channel TMEM16A and CFTR (Figure S6). Next, we assessed cilia coverage and motility as described in Supplementary Materials and Methods. *FOXI1* KO ALI cultures showed a similar CBF to their WT counterparts (Fig. 5C and S4). Intriguingly, the coverage of cilia in *FOXI1* KO epithelia was reduced (Fig. 5D and S4). Although this difference was not statistically significant, it suggested that either the number or function of ciliated cells was decreased in *FOXI1* KO ALI cultures. To distinguish between these possibilities, we performed flow cytometry analyses and observed that the absence of ionocytes resulted in a significant reduction in the number of FOXJ1 expressing cells (Fig. 5E and S5A). The reduced number of ciliated cells in *FOXI1* KO cells was validated with hiPSC-AECs from two other *FOXI1* KO hiPSC clones of the same genetic background (Figure S5B and S5C) and with the clones from the second genetic background (Figure S5D and S5E). Because the FOXJ1+cell number decrease was not as striking in the second genetic background (Figure S5D and S5E), we further investigated this phenotype in CF17/NKX2.1-GFP cells by assessing the expression of mature ciliated cell markers both at protein and mRNA levels. Western blot analysis indicated a decrease of DNAI1 in *FOXI1* KO cells compared to their WT controls (Fig. 5F). RT-qPCR analysis showed decreased expression of the ciliated cell markers *NEK10, DNAH5* and *CP110*, but only the differences in *DNAH5* and *CP110* expression were statistically significant (Figure S5F). Finally, immunofluorescence staining confirmed the presence of FOXJ1+AcTub+ciliated cells in *FOXI1* KO ALI cultures, but these had a more scattered distribution compared to their WT controls (Fig. 5G). Taken together, these results suggest

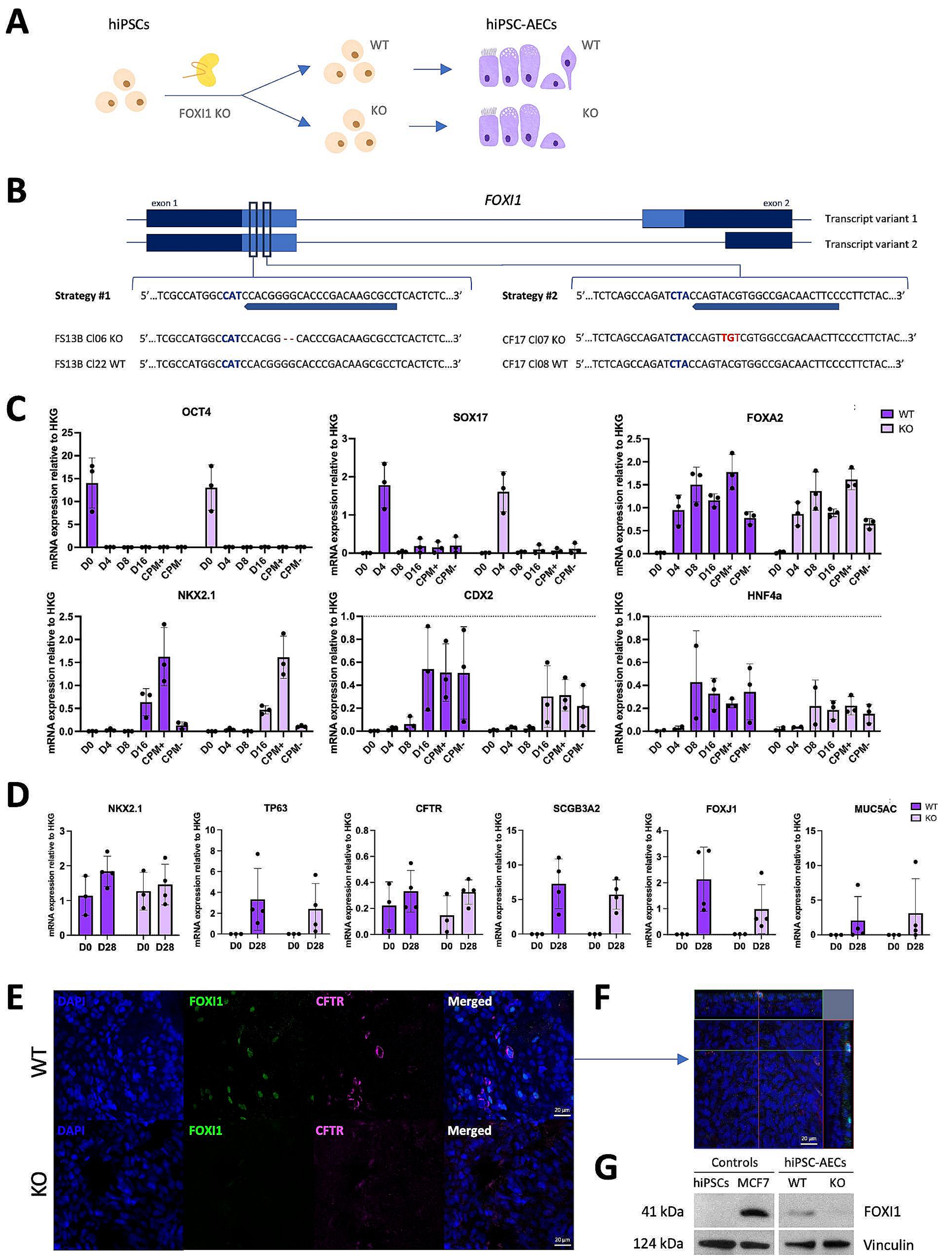

Fig. 4 (See legend on next page.)

(See figure on previous page.)

Fig. 4 *FOXI1* knock-out (KO) in hiPSCs leads to hiPSC-AEC cultures lacking ionocytes. **A**: *FOXI1* gene targeting and differentiation strategy. Following *FOXI1* KO in hiPSCs, WT and KO clones were selected from the targeted pool and differentiated in parallel towards AECs. *FOXI1* KO cells were not expected to generate ionocytes. Targeted but unedited WT cells served as an isogenic control. **B**: Each hiPSC line was targeted with a different sgRNA (Strategy #1 for FS13B and Strategy #2 for CF17/NKX2.1-GFP), testing two different genetic backgrounds and two different targeting strategies in the same study. The diagram shows the sgRNA used on each line to target the DNA binding domain in Exon 1, the PAM region highlighted in blue and the indels in the selected KO clones in red. **C**: Relative mRNA expression of key markers at different time points during the first stages of differentiation. Filled circles represent individual data points and bars are means ± SD ($n=3$ independent experiments); two-way ANOVA with Sidak multiple comparison test. The dotted line indicates the level of the normalized reference-gene expression average value. **D**: Relative mRNA expression of key mature AEC markers of cells in expansion (D0) and after maturation in ALI cultures (D28). Filled circles represent individual data points and bars are means ± SD ($n=3$ independent experiments), two-way ANOVA with Sidak multiple comparison test. **E**: Representative immunocytochemical staining of FOXI1, CFTR and DAPI in mature hiPSC-AECs after 28 days in ALI culture in *FOXI1* WT and KO cells. The scale bar is 20 µm. **F**: Z-stack panel with orthogonal views of *FOXI1* WT cells from E. **G**: Cropped representative Western blot images of FOXI1 expression in WT and KO hiPSC-AECs (right panel), undifferentiated hiPSCs were used as a negative control and MCF7 cells were used as a positive control (left panel). Vinculin was used as a loading control

that ionocytes and/or the expression of *FOXI1* could be involved in the production of functional ciliated cells and could be necessary to establish the normal cellular composition of the lung epithelium.

Discussion

In this study, we described a protocol to differentiate hiPSCs not only into the most abundant cell types of the airway epithelium (basal, ciliated and secretory cells) but also into PNECs and ionocytes. To our knowledge, this is the first report of hiPSC-AECs including these rare cell types in the same culture system.

To date, only one other protocol for hiPSC-AEC differentiation producing ionocytes has been published [8]. In that study, Wang et al. reported the presence of FOXI1+ionocytes using a protocol that requires 3 subsequent sorting steps. Thus, the generation of hiPSC-AEC cultures with ionocytes has proven challenging. One of the reasons for this might be the use of specialised media developed to produce highly ciliated cultures, which probably contain inhibitors of Notch that could reduce the presence of ionocytes [1]. By contrast, our protocol is based on a chemically defined medium combined with short-term culture with PneumaCult™-ALI Medium. This combination leads to hiPSC-AEC cultures that might be less ciliated, but that contain ionocytes expressing FOXI1 and high levels of CFTR or co-expressing FOXI1 and BSND.

We used our hiPSC-AEC cultures to study the impact of *FOXI1* KO on the development and functionality of the airway epithelium. Although ionocytes constitute a rare population in the epithelium, several studies have shown that their impairment can lead to significant phenotypes [1, 2, 12–14]. Consistent with previous results [2], we found that the KO of *FOXI1* does not impact the pH of ASL in ALI cultures. By contrast, we found that *FOXI1* KO impacts R_t values of hiPSC-AEC epithelia. The lower R_t values of *FOXI1* KO epithelia might be due to impaired epithelial barrier function and/or increased numbers/activity of ion channels. According to Pou Casellas et al. [30], transcriptional analysis of ionocytes revealed their involvement in various signalling pathways, including those involving occludin and junctional adhesion molecules, which could potentially explain why their absence affects the formation of a tight epithelial barrier. Additionally, Yuan et al. [15] reported the compensatory overexpression of ion and water channel encoding genes in airway cultures from a *FOXI1* KO ferret model. Although our results differ from those published by Goldfarbmuren et al. [6] and Lei et al. [14], who reported increased R_t in *FOXI1* KO cultures, their data are based on mosaic KOs, while Yuan et al. [15] did not report R_t measurements. The different R_t values of *FOXI1* KO airway epithelia are reminiscent of earlier reports about the effects of the predominant CF-causing *CFTR* variant F508del on R_t. LeSimple et al. [31] found that epithelia heterologously expressing F508del-CFTR had reduced R_t values compared to those expressing wild-type CFTR, whereas Li et al. [32] found the converse. As with these previous studies, differences in the cells studied and the experimental conditions used likely explain the distinct results obtained with *FOXI1* KO airway epithelia.

We found that ALI cultured hiPSC-AECs without ionocytes show reduced cilia motility properties compared to cultures with ionocytes. More importantly, we showed that cultures without ionocytes displayed a smaller number of ciliated cells. This could be the reason for the slower movement of cilia in *FOXI1* KO cultures and it suggests that ionocytes could play a role in mucociliary clearance by influencing the production of ciliated cells. These results do not contradict the previous report by Montoro et al. showing that the absence of Foxi1 in mice led to more viscous mucous secretions in the airway epithelium and, in turn, higher CBF [2]. Our ALI cultured hiPSC-AECs do not produce abundant mucus, and CBF measurements did not change after washing the epithelia with PBS. Therefore, we cannot exclude the possibility that the absence of *FOXI1* expression could also increase mucus viscosity. However, it could be interesting to confirm if the number of ciliated cells is also decreased in a mouse KO for Foxi1. In the study by Goldfarbmuren et al. [6], *FOXI1* KO did not significantly affect *FOXJ1* mRNA expression, consistent with our RT-qPCR results. However, changes in ciliated cell numbers or expression

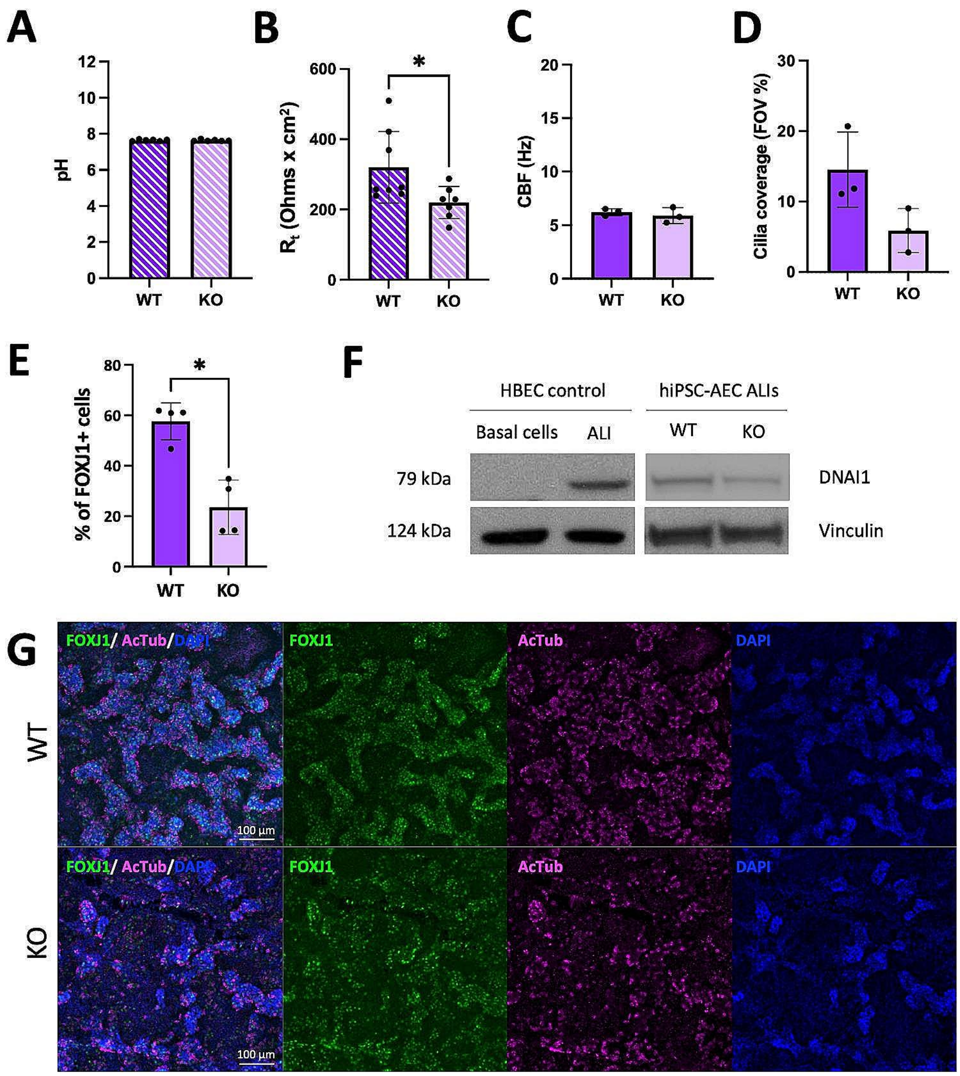

Fig. 5 Functional assays reveal that *FOXI1* KO leads to decreased numbers of ciliated cells in hiPSC-AECs. **A**: Airway surface liquid (ASL) pH of mature *FOXI1* WT and KO hiPSC-AECs. Filled circles represent individual values and bars are means ± SD (n = 6 consists of 3 independent experiments, 2 biological replicates per experiment); Mann-Whitney test. **B**: Transepithelial resistance (R_t) of mature *FOXI1* WT and KO hiPSC-AEC ALI cultures. Filled circles represent the average of 3 technical replicates (measurements) and bars are means ± SD (n = 6 ALIs from 3 independent experiments, 2 biological replicates per experiment). * $P < 0.05$; Mann-Whitney test. **C**: Ciliary beat frequency (CBF) of *FOXI1* WT and KO hiPSC-AEC ALI cultures. Filled circles represent the average of values obtained from 5–20 FOVs with > 5% of coverage from one sample and bars are means ± SD (n = 3 independent experiments); Student's t-test. **D**: Area covered with motile cilia in *FOXI1* WT and KO hiPSC-AEC ALI cultures. Filled circles represent the average of up to 20 FOVs from one sample and bars are means ± SD (n = 3 independent experiments); Student's t-test. **E**: Flow cytometry analysis of the amount of FOXJ1 + ciliated cells in *FOXI1* WT and KO hiPSC-AEC ALI cultures. Gating was performed compared to stained hiPSC controls. Filled circles represent individual values and bars are means ± SD (n = 4 independent experiments); *$P < 0.05$; Mann-Whitney test. **F**: Cropped representative Western blot images show the expression of the ciliated cell marker DNAI1 in mature *FOXI1* WT and KO hiPSC-AECs. Primary basal cells and HBEC ALI cultures served as negative and positive controls, respectively. Vinculin served as a loading control. **G**: Representative immunofluorescence staining of FOXJ1, acetylated tubulin (AcTub) and DAPI in *FOXI1* WT and KO hiPSC-AECs. The scale bar is 100 µm

of key markers at a protein level were not tested in their study. Importantly, our results are reinforced by studies in *Xenopus laevis* epidermis [33] which reported that the almost complete absence of Foxi1 led to a reduced number and aberrant morphology of cilia. Interestingly, engraftment of Foxi1 WT epidermis patches rescued the ciliation of the nearby KO epidermis. Thus, the importance of ionocytes in the production of ciliated cells could be conserved between species and tissues.

Various mechanisms could be driving the decrease of ciliated cells in the absence of FOXI1. First, the KO of *FOXI1* could be directly interfering with differentiation of ciliated cells. However, *FOXI1* is not expressed during the production of these cells [1, 2] and there is no evidence that the lineage of these two cell types is interdependent even if they both originate from basal cells [2, 6]. Second, cell-to-cell contact could be necessary between ionocytes and ciliated cells for the proper differentiation of the latter. This hypothesis would fit with the results obtained with *Xenopus laevis* epidermis [33]. Furthermore, ionocyte and ciliated cell differentiation is tightly controlled by Notch signalling. Thus, Notch-related crosstalk between the two cell types could play a role in the maturation of ciliated cells. Finally, it has been shown that ion channels and transporters highly expressed in ionocytes, such as the VATPase, are important in the regulation of Wnt signalling [34–36]. Interestingly, canonical Wnt/beta-catenin signalling has a role in the activation of the cilia development machinery via the regulation of *FOXJ1* expression [37–39], while the Wnt planar cell polarity signalling pathway is responsible for actin organisation and cilia beat alignment and coordination [40, 41]. The lack of ionocytes could affect the acidification of the microenvironment thereby blocking Wnt signalling and ciliated cell differentiation. Further investigation of AECs will help elucidate how such pathways can be controlled by pulmonary ionocytes.

Conclusion

Overall, our study confirms that hiPSCs can be differentiated into an airway epithelium containing ionocytes and that *FOXI1* KO leads to a depletion of these cells. We show that the absence of ionocytes leads to impairment of epithelial barrier properties and ciliated cell homeostasis, revealing their potential role in the formation of the airway epithelium. This information represents an important step toward understanding the function of these cells in normal homeostasis and in lung disease, paving the way for new therapeutic applications focusing on ionocytes control.

Abbreviations

AcTub	acetylated tubulin
AEC	airway epithelial cell
ALI	air liquid interface
ASCL1	achaete-scute family bHLH transcription factor 1
ASCL3	achaete-scute family bHLH transcription factor 3
ASL	airway surface liquid
BSND	barttin CLCNK type accessory subunit beta
CBF	ciliary beat frequency
CF	cystic fibrosis
CFTR	cystic fibrosis transmembrane conductance regulator
CK5	cytokeratin 5
CPM	carboxypeptidase-M
CP110	centrosomal protein of 110 kDa
CRISPR	clustered regularly interspaced short palindromic repeats
DAPT	(2 S)-N-[2(3,5-Difluorophenyl)acetyl]-L-alanyl-2-phenyl-glycine 1,1-Dimethylethyl ester
DNAI1	dynein axonemal intermediate chain 1
DNAH5	dynein axonemal heavy chain 5
FGF10	fibroblast growth factor 10
FOV	field of view
FOXI1	forkhead box I1
FOXJ1	forkhead box J1
GCRP	calcitonin gene-related peptide
GFP	green fluorescent protein
hiPSC	human induced pluripotent stem cell
HBEC	human bronchial epithelial cell
hiPSC-AECs	human induced pluripotent stem cell-derived airway epithelial cells
HKG	housekeeping gene
I_{SC}	short circuit current
KO	knock-out
mRNA	messenger RNA
MUC5AC	mucin 5AC
NEK10	NIMA related kinase 10
NKX2.1	NK2 homeobox 1
PBS	phosphate-buffered saline
PNEC	pulmonary neuroendocrine cell
R_t	transepithelial resistance
RT-qPCR	reverse transcription-quantitative polymerase chain reaction
SAG	Smoothened agonist
SCGB3A2	secretoglobin family 3 A member 2
sgRNA	single guide RNA
SOX2	SRY-box transcription factor 2
STAP1	signal transducing adaptor family member 1
TP63	tumour protein p63
WT	wild-type

Supplementary Information

The online version contains supplementary material available at https://doi.org/10.1186/s12931-024-02800-7.

Supplementary Material 1

Supplementary Material 2

Supplementary Material 3

Acknowledgements

We thank UTHEALTH and Jed Mahoney, Megan Peasley and the scientists at the Cystic Fibrosis Foundation for the gift of the CF17/NKX2.1-GFP human hiPSC line and Scott H. Randell of the University of North Carolina for his advice on ALI cultures. We are also thankful to Anna Osnato, from the Cambridge Stem Cell Institute, for her input in cell sorting experiments. **'This research was funded in whole, or in part, by the Wellcome Trust [203151/Z/16/Z] and the UKRI Medical Research Council [MC_PC_17230]. For the purpose of open access, the authors have applied a CC BY public copyright licence to any Author Accepted Manuscript version arising from this submission.'**

Author contributions

MVG: Study design, experiment execution, data analysis and interpretation, manuscript writing; LPi: Experiment execution, data analysis and interpretation; RF: Experiment execution, code development, data analysis; EC: Experiment execution, code development, data analysis; HK: In vivo experiment execution, data analysis; MR: Experiment design, experiment execution, data analysis and interpretation; CMM: Generation of GFP hiPSC reporter line; MAT: Experiment execution; LPo: Experiment execution; WG: Experiment execution; RM: Experiment execution; SLH: Experiment design; FM: Experiment design; AG: Experiment design; DNS: Experiment design, data analysis and interpretation, manuscript revision; RAF: Experiment design; ELR: In vivo experiment design and execution, data analysis, manuscript revision; PC: Code development, experiment design; LV: Study design, data analysis, manuscript writing; All authors: reviewing and approval of the final version of the manuscript.

Funding

This work was supported by the Wellcome Trust Sir Henry Wellcome Postdoctoral Fellowship (218663/Z/19/Z to MVG), the UK Cystic Fibrosis Trust (IH001 to MVG, RAF; SRC 016 to LPi, RF, PC; SRC 021 to DNS; VIA 028 to HK, ELR; RM, SLH), the EU ITN PhyMot (to EC), the European Research Council Grant New-Chol (ERC: 741707 to LV), the MRC (MR/P009581/1 to HK, ELR), the Medical Research Foundation Fellowship (to MA-T, AG), the NC3Rs (Training Fellowship NC/R001987/1 to CMM; Project Grant NC/S001204/1 to LPo, WG, FM), the Roy Castle Lung Cancer Foundation grant (2015/10/McCaughan to

LPo, WG, FM), the Biotechnology and Biological Science Research Council (BB/W014564/1 to FM and WG), the Cystic Fibrosis Foundation (to RM, SLH) and the core support grant from the Wellcome Trust (203151/Z/16/Z) and the UKRI Medical Research Council (MC_PC_17230) for the Wellcome MRC – Cambridge Stem Cell Institute. This paper presents independent research supported by the NIHR Cambridge BRC. The NIHR Cambridge Biomedical Research Centre (BRC) is a partnership between Cambridge University Hospitals NHS Foundation Trust and the University of Cambridge, funded by the National Institute for Health Research (NIHR). The views expressed are those of the author(s) and not necessarily those of the NIHR or the Department of Health and Social Care.

Data availability

The single guide RNA and RT-qPCR primer sequences used for this study are provided in the Supplementary Materials and Methods. The code used to analyse cilia motility and coverage is publicly available [26] and the obtained data can be found in the Zenodo repository (DOI: https://doi.org/10.5281/zenodo.8309970). Other datasets and materials used and/or analysed in this study are available from the corresponding authors on reasonable request.

Declarations

Ethics approval and consent to participate

All animal experiments were approved by local ethical review committees and conducted according to Home Office project license PPL PEEE9B8E4 (Emma L. Rawlins, University of Cambridge).

Consent for publication

Not applicable.

Competing interests

The authors declare no competing interests.

Author details

[1]Wellcome-MRC Cambridge Stem Cell Institute, Jeffrey Cheah Biomedical Centre, University of Cambridge, Puddicombe Way, Cambridge CB2 0AW, UK
[2]Department of Physics, Cavendish Laboratory, University of Cambridge, JJ Thomson Avenue, Cambridge CB3 0HE, UK
[3]Wellcome Trust/CRUK Gurdon Institute, University of Cambridge, Tennis Court Road, Cambridge CB2 1QN, UK
[4]School of Physiology, Pharmacology and Neuroscience, Biomedical Sciences Building, University of Bristol, University Walk, Bristol BS8 1TD, UK
[5]Center of Research and Development for Biomedical Instrumentation, Institute of Molecular Biosciences, Mahidol University, Nakhon Pathom 73170, Thailand
[6]IRCCS Humanitas Research Hospital, via Manzoni 56, Rozzano, Milan 20089, Italy
[7]Department of Clinical Neurosciences, Victor Phillip Dahdaleh Heart & Lung Research Institute, University of Cambridge, Papworth Road, Cambridge CB2 0BB, UK
[8]Department of Medicine, Victor Phillip Dahdaleh Heart & Lung Research Institute, University of Cambridge, Papworth Road, Cambridge CB2 0BB, UK
[9]Genetics and Genome Medicine Department, UCL Great Ormond Street Institute of Child Health, London WC1N 1EH, UK
[10]Molecular Immunity Unit, Department of Medicine, University of Cambridge, Cambridge CB2 0QH, UK
[11]Cambridge Centre for Lung Infection, Royal Papworth Hospital NHS Foundation Trust, Cambridge CB2 0AY, UK
[12]Department of Physiology, Development and Neuroscience, University of Cambridge, Tennis Court Road, Cambridge CB2 1QN, UK
[13]BIH Center for Regenerative Therapies, Berlin Institute of Health at Charité, Augustenburger Platz 1, 13353 Berlin, DE, Germany
[14]Max Planck Institute for Molecular Genetics, Ihnestraße 63-73, 14195 Berlin, Germany
[15]Cell Therapy and Tissue Engineering Group, Research Institute of Health Sciences (IUNICS), University of Balearic Islands, Palma 07122, Spain
[16]Health Research Institute of the Balearic Islands (IdISBa), Palma 07120, Spain

Received: 3 September 2023 / Accepted: 1 April 2024
Published online: 25 April 2024

References

1. Plasschaert LW, Žilionis R, Choo-Wing R, Savova V, Knehr J, Roma G, et al. A single-cell atlas of the airway epithelium reveals the CFTR-rich pulmonary ionocyte. Nature. 2018;560(7718):377–81.
2. Montoro DT, Haber AL, Biton M, Vinarsky V, Lin B, Birket SE, et al. A revised airway epithelial hierarchy includes CFTR-expressing ionocytes. Nature. 2018;560(7718):319–24.
3. Engelhardt JF, Yankaskas JR, Ernst SA, Yang Y, Marino CR, Boucher RC, et al. Submucosal glands are the predominant site of CFTR expression in the human bronchus. Nat Genet. 1992;2(3):240–8.
4. Scudieri P, Musante I, Venturini A, Guidone D, Genovese M, Cresta F, et al. Ionocytes and CFTR Chloride Channel expression in normal and cystic fibrosis nasal and bronchial epithelial cells. Cells. 2020;9(9):2090.
5. Okuda K, Dang H, Kobayashi Y, Carraro G, Nakano S, Chen G, et al. Secretory cells dominate Airway CFTR expression and function in human airway superficial epithelia. Am J Respir Crit Care Med. 2021;203(10):1275–89.
6. Goldfarbmuren KC, Jackson ND, Sajuthi SP, Dyjack N, Li KS, Rios CL, et al. Dissecting the cellular specificity of smoking effects and reconstructing lineages in the human airway epithelium. Nat Commun. 2020;11(1):2485.
7. Quigley IK, Stubbs JL, Kintner C. Specification of ion transport cells in the Xenopus larval skin. Development. 2011;138(4):705–14.
8. Wang R, Simone-Roach C, Lindstrom-Vautrin J, Wang F, Rollins S, Bawa PS, et al. De Novo Generation of Pulmonary ionocytes from normal and cystic Fibrosis Human Induced Pluripotent Stem cells. Am J Respir Crit Care Med. 2023;207(9):1249–53.
9. Tsao PN, Vasconcelos M, Izvolsky KI, Qian J, Lu J, Cardoso WV. Notch signaling controls the balance of ciliated and secretory cell fates in developing airways. Development. 2009;136(13):2297–307.
10. Serra CFH, Liu H, Qian J, Mori M, Lu J, Cardoso WV. Prominin 1 and Notch regulate ciliary length and dynamics in multiciliated cells of the airway epithelium. iScience. 2022;25(8):104751.
11. Walentek P. Signaling Control of Mucociliary Epithelia: stem cells, cell fates, and the plasticity of cell identity in Development and Disease. Cells Tissues Organs. 2022;211(6):736–53.
12. Cai Q, Luo M, Tang Y, Yu M, Yuan F, Gasser GN, et al. Sonic hedgehog signaling is essential for pulmonary ionocyte specification in human and ferret Airway Epithelia. Am J Respir Cell Mol Biol. 2023;69(3):295–309.
13. Sato Y, Kim D, Turner MJ, Luo Y, Zaidi SSZ, Thomas DY, et al. Am J Respir Cell Mol Biol. 2023;69(3):281–94. https://doi.org/101165/rcmb2022-0241OC. Ionocyte-Specific Regulation of CFTR.
14. Lei L, Traore S, Ibarra GSR, Karp PH, Rehman T, Meyerholz DK, et al. CFTR-rich ionocytes mediate chloride absorption across airway epithelia. J Clin Invest. 2023;133(20):e171268.
15. Yuan F, Gasser GN, Lemire E, Montoro DT, Jagadeesh K, Zhang Y, et al. Transgenic ferret models define pulmonary ionocyte diversity and function. Nature. 2023;621(7980):857–67.
16. Jonz MG, Nurse CA. Epithelial mitochondria-rich cells and associated innervation in adult and developing zebrafish. J Comp Neurol. 2006;497(5):817–32.
17. Konishi S, Gotoh S, Tateishi K, Yamamoto Y, Korogi Y, Nagasaki T, et al. Directed induction of functional multi-ciliated cells in Proximal Airway Epithelial spheroids from Human pluripotent stem cells. Stem cell Rep. 2016;6(1):18–25.
18. Hawkins FJ, Suzuki S, Beermann M, Lou, Barillà C, Wang R, Villacorta-Martin C, et al. Derivation of Airway basal stem cells from human pluripotent stem cells. Cell Stem Cell. 2021;28(1):79–e958.
19. Hein RFC, Conchola AS, Fine AS, Xiao Z, Frum T, Brastrom LK, et al. Stable iPSC-derived NKX2-1 + lung bud tip progenitor organoids give rise to airway and alveolar cell types. Development. 2022;149(20):dev200693.
20. Hor P, Punj V, Calvert BA, Castaldi A, Miller AJ, Carraro G, et al. Efficient generation and transcriptomic profiling of human iPSC-Derived pulmonary neuroendocrine cells. iScience. 2020;23(5):101083.
21. Kilpinen H, Goncalves A, Leha A, Afzal V, Alasoo K, Ashford S, et al. Common genetic variation drives molecular heterogeneity in human iPSCs. Nature. 2017;546(7658):370–5.
22. McCauley KB, Hawkins F, Serra M, Thomas DC, Jacob A, Kotton DN. Efficient derivation of functional human airway epithelium from pluripotent stem cells via temporal regulation of wnt signaling. Cell Stem Cell. 2017;20(6):844–e8576.

23. Ishikawa F, Yasukawa M, Lyons B, Yoshida S, Miyamoto T, Yoshimoto G, et al. Development of functional human blood and immune systems in NOD/SCID/IL2 receptor {gamma} chain(null) mice. Blood. 2005;106(5):1565–73.
24. Shultz LD, Lyons BL, Burzenski LM, Gott B, Chen X, Chaleff S, et al. Human lymphoid and Myeloid Cell Development in NOD/LtSz-scid IL2Rγnull mice engrafted with mobilized human hemopoietic stem cells. J Immunol. 2005;174(10):6477–89.
25. Leung C, Wadsworth SJ, Jasemine Yang S, Dorscheid DR. Structural and functional variations in human bronchial epithelial cells cultured in air-liquid interface using different growth media. Am J Physiol - Lung Cell Mol Physiol. 2020;318(5):L1063–73.
26. Fradique R, Causa E, Delahousse C, Kotar J, Pinte L, Vallier L, et al. Assessing motile cilia coverage and beat frequency in mammalian in vitro cell culture tissues. R Soc open Sci. 2023;10(8):230185.
27. Miller AJ, Hill DR, Nagy MS, Aoki Y, Dye BR, Chin AM, et al. In Vitro induction and in vivo Engraftment of Lung Bud Tip Progenitor cells derived from human pluripotent stem cells. Stem Cell Rep. 2018;10(1):101–19.
28. Ikeo S, Yamamoto Y, Ikeda K, Sone N, Korogi Y, Tomiyama L, et al. Core-shell hydrogel microfiber-expanded pluripotent stem cell-derived lung progenitors applicable to lung reconstruction in vivo. Biomaterials. 2021;276:121031.
29. Ma L, Thapa BR, Suer JA, Le, Tilston-Lünel A, Herriges MJ, Berical A, et al. Airway stem cell reconstitution by the transplantation of primary or pluripotent stem cell-derived basal cells. Cell Stem Cell. 2023;30(9):1199–e12617.
30. Pou Casellas C, Pleguezuelos-Manzano C, Rookmaaker MB, Verhaar MC, Clevers H. Transcriptomic profile comparison reveals conservation of ionocytes across multiple organs. Sci Rep. 2023;13(1):3516.
31. LeSimple P, Liao J, Robert R, Gruenert DC, Hanrahan JW. Cystic fibrosis transmembrane conductance regulator trafficking modulates the barrier function of airway epithelial cell monolayers. J Physiol. 2010;588(Pt 8):1195–209.
32. Li H, Yang W, Mendes F, Amaral MD, Sheppard DN. Impact of the cystic fibrosis mutation F508del-CFTR on renal cyst formation and growth. Am J Physiol Ren Physiol. 2012;303(8):F1176–86.
33. Dubaissi E, Papalopulu N. Embryonic frog epidermis: a model for the study of cell-cell interactions in the development of mucociliary disease. Dis Model Mech. 2011;4(2):179–92.
34. Cruciat CM, Ohkawara B, Acebron SP, Karaulanov E, Reinhard C, Ingelfinger D, et al. Requirement of prorenin receptor and vacuolar H+-ATPase-mediated acidification for wnt signaling. Science. 2010;327(5964):459–63.
35. Sun DI, Tasca A, Haas M, Baltazar G, Harland RM, Finkbeiner WE, et al. Na+/H + exchangers are required for development and function of vertebrate mucociliary epithelia. Cells Tissues Organs. 2018;205(5–6):279–92.
36. Walentek P, Beyer T, Hagenlocher C, Müller C, Feistel K, Schweickert A, et al. ATP4a is required for development and function of the Xenopus mucociliary epidermis - a potential model to study proton pump inhibitor-associated pneumonia. Dev Biol. 2015;408(2):292–304.
37. Walentek P, Beyer T, Thumberger T, Schweickert A, Blum M. ATP4a is required for wnt-dependent Foxj1 expression and Leftward Flow in Xenopus Left-Right Development. Cell Rep. 2012;1(5):516–27.
38. Stubbs JL, Oishi I, Izpisúa Belmonte JC, Kintner C. The forkhead protein Foxj1 specifies node-like cilia in Xenopus and zebrafish embryos. Nat Genet. 2008;40(12):1454–60.
39. Caron A, Xu X, Lin X. Wnt/β-catenin signaling directly regulates Foxj1 expression and ciliogenesis in zebrafish Kupffer's vesicle. Development. 2012;139(3):514–24.
40. Vladar EK, Antic D, Axelrod JD. Planar Cell Polarity Signaling: the developing cell's compass. Cold Spring Harb Perspect Biol. 2009;1(3):a002964.
41. Wallingford JB. Planar cell polarity signaling, cilia and polarized ciliary beating. Curr Opin Cell Biol. 2010;22(5):597–604.

Publisher's Note